Jestr

Journal of Engineering Science and Technology Review 16 (6) (2023) 54 - 62

Research Article

JOURNAL OF
Engineering Science and Technology Review

www.jestr.org

Indirect Tensile Properties of Basalt Fiber-reinforced Recycled Aggregate Concrete after Elevated Temperature Exposure

Xianggang Zhang[1, 2], Youchuan Shen[2, *], Chengyi Luo[2] and Yajun Huang[1]

[1]*School of Intelligent Construction, Wuchang University of Technology, Wuhan 430223, China*
[2]*School of Civil Engineering, Henan Polytechnic University, Jiaozuo 454003, China*

Received 12 August 2023; Accepted 27 November 2023

Abstract

With recycled coarse aggregate replacement ratio, basalt fiber (BF) dosage, and exposure temperature as variation parameters, 162 specimens were designed and fabricated to examine the influence of elevated temperature exposure on the indirect tensile properties of basalt fiber-reinforced recycled aggregate concrete (BFRRC). The BFRRC specimens underwent splitting tensile and flexural tests after exposure to an elevated temperature. The failure modes of the specimens were observed and the effects of the variation parameters on the indirect tensile properties of BFRRC were analyzed. Simultaneously, the interrelationships among splitting tensile strength, flexural strength, and cubic compressive strength were examined. Results show that, the functional correlations among the aforementioned strength indices are determined. The temperature exerts the greatest influence on the failure mode of BFRRC. In addition, the inclusion of fibers improves the damage degree, while the effect of replacement ratio is insignificant. The mechanical properties of BFRRC, including its indirect tensile strength, exhibit a decrease with increasing replacement ratio and temperature. Conversely, an increase in fiber dosage enhances these qualities. The conclusions obtained in this study provide a reference to the application of BFRRC.

Keywords: Recycled aggregate concrete, Basalt fiber, Elevated temperature, Indirect tensile strength, Mechanical properties

1. Introduction

Concrete is highly regarded and extensively utilized in civil engineering due to its exceptional performance characteristics, making it one of the most prevalent building materials. In recent years, modern urbanization processes have led to the demolition of numerous old buildings, generating substantial quantities of concrete waste [1]. Currently, disposal methods that are commonly employed for unwanted concrete involve either subsurface landfills or haphazard open-air stacking [2]. The aforementioned treatment methods not only result in significant environmental degradation but also pose numerous challenges to subsequent production and development endeavors, deviating entirely from the principles of sustainable development. The utilization of waste concrete as recycled aggregate in manufactured recycled aggregate concrete offers a feasible solution to the aforementioned issues [3, 4]. However, the inferior mechanical properties of recycled aggregate concrete (RAC) compared with those of regular concrete impose constraints on the feasible technical utilization of RAC [5, 6]. Hence, the identification of appropriate methodologies for augmenting the mechanical properties of RAC is imperative to facilitate its widespread utilization.

To mitigate the adverse effects of internal faults in recycled coarse aggregate (RCA) on RAC, scholars have devised various methods for augmenting the mechanical properties of RAC. These strategies mostly involve the elimination and reinforcement of mortar on RCA surfaces [7]. The process used in surface mortar removal pertains to the elimination of the initial mortar that is present over the surface of RCA by using physical or chemical means. This process involves techniques such as mechanical grinding, presoaking with acid solutions, and presoaking with water [8-10]. The reinforced surface mortar technique encompasses the application of specialized treatment methods that produce carbonates, gels, and other compounds on the surface of RCA mortar. These chemical compounds fill pores and cracks in the mortar. Notable treatment methods include carbonization, nanomaterial technology, and volcanic slurry treatment [11-13]. The aforementioned techniques have the potential to mitigate the inherent deficiencies of RCA while effectively enhancing the mechanical properties of RAC. However, such approaches are not without limitations, which include higher costs, prolonged time requirements, environmental pollution, and limited scalability. Hence, more efficient and environmentally sound methods must be used for augmenting the mechanical properties of RAC.

Research has revealed that the utilization of fiber-reinforced concrete (FRC) can be a viable approach for enhancing the mechanical properties of concrete. Moreover, adding some types of fibers to concrete has been found to impede crack initiation and propagation, contributing toward the improvement of the overall strength and ductility of materials [14, 15]. Basalt fiber (BF) is a novel material that exhibits environmental sustainability and exceptional performance characteristics. It possesses notable features, such as a high elastic modulus and excellent compatibility with concrete [18]. Hence, the inclusion of BF with RAC has resulted in improved mechanical properties compared with those of RAC alone. Presently, domestic and international academics are conducting an increasing amount of research on BF-reinforced RAC (BFRRC). However,

*E-mail address: shenyouchuan@163.com
ISSN: 1791-2377
doi:10.25103/jestr.166.07

studies on the mechanical properties of BFRRC after exposure to an elevated temperature are less. The present work conducts an experimental study on indirect tensile mechanical properties after exposure to elevated temperature conditions associated with BFRRC. The findings of this study present valuable and worthwhile insights into the fire protection design of BFRRC.

2. State of the art

A significant number of scholarly studies have been conducted on FRC in recent years. Shi et al. [17] examined the basic characteristics of steel FRC treated under uniaxial compression and tensile conditions with various fiber dosages. Their findings indicated that integrating fibers into concrete led to a notable enhancement in its tensile strength and an improvement in its tensile toughness and compressive toughness. The flexural performance of carbon FRC beams subjected to impaction load was investigated by Wang et al. [18], who researched about the effects of varying fiber dosages. Their findings indicated that the beam exhibited the highest energy absorption capacity at a fiber dosage of 0.35%. Zhu et al. [19] examined the effect of alkali-resistant glass fiber on the strength of concrete. Their results indicated that when the glass fiber content was 1 %, the tensile strength and peak strength of concrete were the highest. Sainz-Aja et al. [20] recycled polyethylene fiber from waste and examined the effect of fiber on the performance of concrete. Their findings indicated that incorporating fibers improved the tensile strength of concrete, and the effect of concrete with higher fiber dose was more obvious. The influences of glass and polypropylene fibers on the mechanical properties of concrete were examined by Liu et al. [21]. Their findings demonstrated that the flexural and compressive characteristics of concrete with fibers were notably superior to those of conventional concrete. Furthermore, the combined use of two types of fibers exerted a more pronounced enhancement effect compared with using only one type of fibers. The effects of varying doses of steel and polypropylene fibers on the mechanical properties of concrete after elevated temperature exposure were reported by Bošnjak et al. [22]. Their findings identified that the existence of fibers increased the splitting tensile strength and flexural strength of concrete by 40% to 150%. In summary, prior research has demonstrated that fibers exhibit the ability to restrict crack propagation through the mechanisms of bridging and crack resistance. Moreover, certain types of fibers that may augment the mechanical properties of concrete to a certain degree have been identified. With developments in research, researchers have made a significant discovery that pertained to a novel variety of inorganic green fiber, referred to as BF. In addition to possessing the characteristics of various fiber bridging and cracking-resistance mechanisms, BF exhibits several advantageous traits compared with alternative fibers. These traits include higher chemical durability than steel fibers, reduced cost compared with carbon fibers, and enhanced adhesion to cement compared with polypropylene [23-25]. Consequently, focus on BF has been increasing, leading to extensive studies on BFRRC.

Dong et al. [26] exhibited a negative correlation between the replacement ratio of RCA and the stiffness and bearing capacity of RAC columns. Conversely, they observed a positive relationship between the dosage of BF slag and the stiffness and bearing capacity of RAC columns. Zhang et al. [27] reported that the compressive strength of BFRRC was negatively correlated with the ratio of RCA replacement. Conversely, an increase in BF dosage was found to positively affect compressive strength. Furthermore, their study revealed that RCA replacement ratio exerted a more significant effect on BFRRC strength. Shatarat et al. [28] conducted an investigation into the bond strength of BFRRC. Their findings revealed a notable rise in the bond strength of BFRRC when BF dosage was increased. Zhang et al. [29] analyzed the fundamental strength index for BFRRC and established the conversion relationship among different strength indices. A bending examination of beams made of BFRRC with varying replacement ratios of RCA was performed by Li et al. [30]. Their findings indicated the insignificant effect of RCA admixture on the flexural strength of concrete. Conversely, incorporating fibers resulted in a substantial enhancement of its flexural strength. Simultaneously, integrating fibers into concrete diminishes crack propagation while enhancing its ductile properties. Zhang et al. [31] conducted a comprehensive set of experiments to evaluate the fundamental mechanical properties of BFRRC. Their findings demonstrated that as BF content grew, the strength of BFRRC progressively increased with a 50% replacement ratio, surpassing that of concrete with alternative replacement ratios. This outcome substantiated the viability of the suggested approach for generating RAC. The mechanical properties and durability of BFRRC were investigated by Chen et al. [32]. Their findings showed that the incorporation of BF exhibited the potential for enhancing the mechanical properties of RAC while concurrently decreasing its porosity and enhancing its resistance to chloride ion ingress.

The existing studies have mostly focused on examining the mechanical properties and durability of BFRRC under ambient conditions. By contrast, the studies that examined its performance after exposure to extreme temperatures are limited. The current study aimed to examine the splitting tensile and flexural properties of BFRRC by varying RCA replacement ratio, BF dosage, and temperature. The analysis focused on understanding the effects of each variation parameter on the indirect tensile strength properties of BFRRC. The findings serve as a crucial foundation for future research on BFRRC.

The rest of this study is organized as follows. Section 3 gives the test material, mix proportions of RAC, specimen design and production, and test method. Section 4 describes the results and discussion, and finally, the conclusions are summarized in Section 5.

3. Methodology

3.1 Test material

The natural coarse aggregate (NCA) consisted of crushed stone, while the RCA was produced by using crushers to break up waste concrete pavement. The fine aggregate (FA) utilized in this study was natural yellow sand. Table 1 provides the fundamental performance indexes of the coarse and fine aggregates. The fiber utilized chopped BF as its primary material, and the corresponding performance indicators are presented in Table 2. Ordinary P·O 42.5R grade cement was used for the tests. The measured fineness was 1.3%, the loss of ignition was 2.4%, compressive strength was 50 MPa, flexural strength was 8 MPa, and the initial/final setting times were 185/270 min. Fly ash (FA)

(Grade II, fineness: 45 μm, density: 2.4 g/cm^3, water content: 0.25%, and loss of ignition: 2.4%), which constituted 20% of the cement dosage, was also employed. A brown-yellow solid water reducer, with a water-reducing efficiency ranging from 15% to 25%, was used. The recommended dosage was 0.5% of the cementitious material, which consisted of cement and fly ash. The water tested was sourced from an urban tap.

Table 1. Fundamental characteristics of aggregates.

Aggregate category	NCA	RCA	FA
Bulk density (kg·m^{-3})	1681	1274	2600
Apparent density (kg·m^{-3})	2798	2433	1300
Moisture content (%)	0.7	1.8	–
Water absorption (%)	0.1	3.5	–
Porosity (%)	–	–	50.29
Crush index	10.4	12.7	–
Particle size (mm)	5-30	5-30	–
Fineness modulus	–	–	2.16

Table 2. Basic properties of BF.

Density (kg·m^{-3})	**Outer diameter (μm)**	**Length (mm)**	**Tensile strength (GPa)**	**Elastic modulus (MPa)**	**Elongation at break (%)**
2650	15	18	104	4500	3.1

3.2 Mix proportions of RAC

The experimental investigation involved the testing of BFRRC with a compressive strength of C40, as specified in the Specification for the Mix Proportion Design of Ordinary Concrete (China JGJ55-2011). First, a suitable water-binder ratio was established and the quantities available in every material were quantified. Subsequently, the ratio should be designed based on the percentage of RCA compared with the total mass of the coarse aggregate. This design should be implemented for three replacement ratios: 0%, 50%, and 100%. In addition, the amount of additional water, the quantity of RCA, and its moisture content and water absorption capacity should be considered. The mix proportion design for testing with RAC is presented in Table 3.

Table 3. Mix proportions of RAC.

δ (%)	W/B	S_s (%)	m_w		m_B		m_A		m_s	m_{wr}
			m_{nw}	m_{aw}	m_c	m_{FA}	m_r	m_n		
0	0.47	32	191	0.00	346	60.9	0.0	1224.9	577	2.04
50	0.47	32	191	10.23	346	60.9	612.4	612.4	577	2.04
100	0.47	32	191	20.45	346	60.9	1224.9	0.0	577	2.04

Note: W/B indicates water-to-binder ratio. δ indicates the replacement ratio of RCA. S_s indicates the sand ratio. m_{nw} and m_{aw} indicate the amount of net water and the mass of additional water, respectively. m_B and m_A represent the masses of the cementitious materials and coarse aggregate, respectively. m_c and m_{FA} represent the masses of cement and FA, respectively. m_r and m_n represent the masses of RCA and NCA, respectively. m_s and m_{wr} represent the masses of FA and the water reducer, respectively.

3.3 Specimen design and production

To study the effects of the replacement ratio of RCA (denoted as δ), BF dosage (denoted as λ), and temperature (denoted as T) on the mechanical properties of BFRRC in indirect tensile testing, 27 specimen groups were meticulously created. The RCA replacement ratio encompassed three distinct functional states: 0%, 50%, and 100%. Similarly, BF dosage encompassed three functional states: 0, 2, and 4 kg·m^{-3}. Lastly, temperature encompassed three functional states: 25 °C, 300 °C, and 600 °C. For conducting the splitting tensile strength test, 81 standard cube specimens with a side length of 150 mm were prepared. In addition, 81 standard prism specimens with dimensions of 150 mm × 150 mm × 550 mm were fabricated specifically for conducting the flexural strength test.

In accordance with the guidelines outlined in the Standard for Test Methods of Physical and Mechanical Properties of Concrete (China GB/T50081-2019), concrete specimens were fabricated using standardized molds. After pouring, the specimens were subjected to dense vibrations and subsequently smoothed. After being left undisturbed overnight, the specimens were carefully removed from the molds and uniformly positioned within a designated curing room. The curing room environment was maintained at an appropriate temperature of 20 ± 2 °C and humidity percentage of more than 95%, ensuring the desired quality of specimen formation. Upon the completion of the 28-day curing period, the aforementioned test was promptly conducted to maintain the precision of the collected data.

3.4 Test method

The indirect tensile mechanical properties of the standard BFRRC specimens were evaluated after exposure to different elevated temperatures. The experimental setup for testing these properties is shown in Fig. 1. In accordance with China's GB/T50081-2019 standard, experiments for determining the splitting tensile strength and flexural strength were conducted using a loading rate of 0.06 MPa/s.

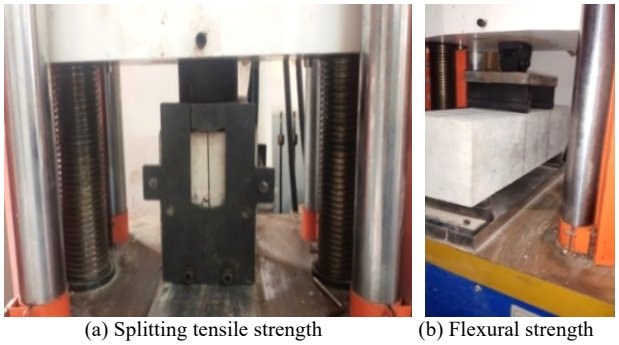

(a) Splitting tensile strength (b) Flexural strength

Fig. 1. Loading device.

4. Results analysis

4.1 Failure process and modes

4.1.1 Splitting tensile failure

Fig. 2 depicts the splitting tensile failure modes of partial specimens. No notable alterations were observed on the surfaces of the specimens until the splitting load reached its maximum magnitude. Upon reaching the designated loading amount, the surfaces of the specimens, which were kept at room temperature, divided into two halves after the quick development of a crack along the loading direction at the center of the surface.

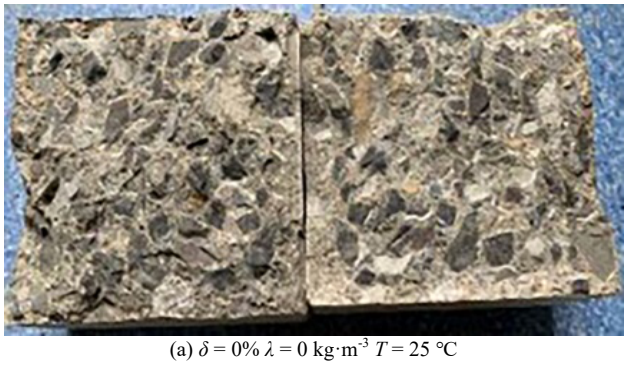

(a) δ = 0% λ = 0 kg·m^{-3} T = 25 ℃

(b) δ = 100% λ = 4 kg·m^{-3} T = 25 ℃

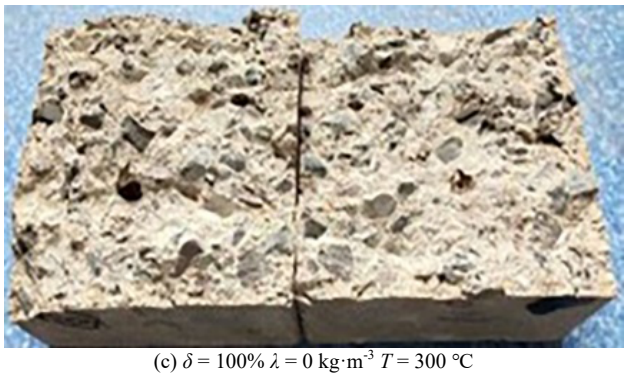

(c) δ = 100% λ = 0 kg·m^{-3} T = 300 ℃

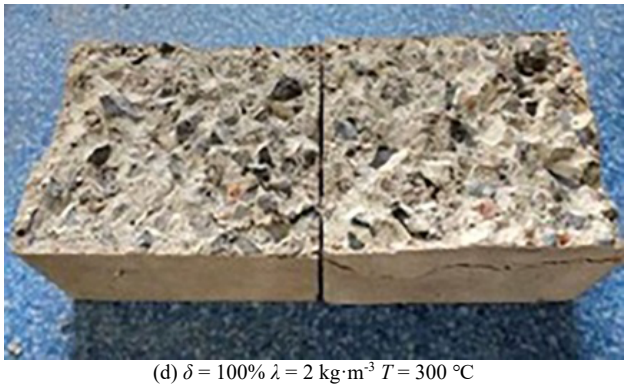

(d) δ = 100% λ = 2 kg·m^{-3} T = 300 ℃

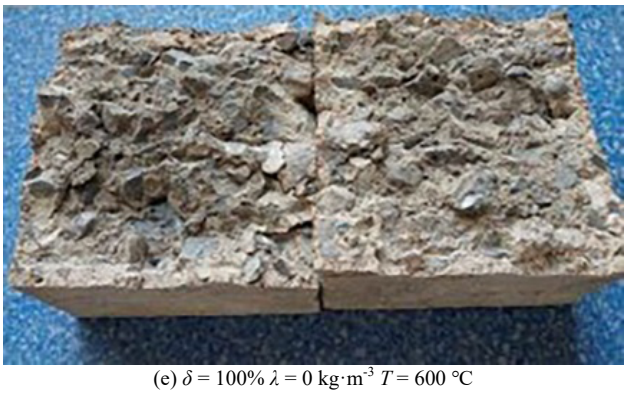

(e) δ = 100% λ = 0 kg·m^{-3} T = 600 ℃

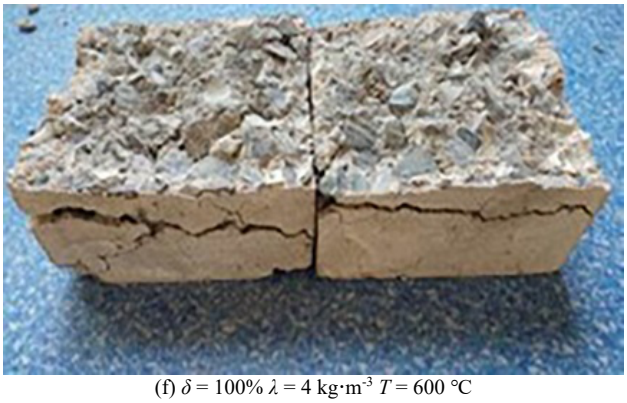

(f) δ = 100% λ = 4 kg·m^{-3} T = 600 ℃

Fig. 2. Splitting tensile failure modes of partial specimens.

The detachment of aggregate and mortar from the affected area, which led to the partial separation of the aggregate, characterized the abrupt occurrence of the failure event. After exposure to 300 °C, the damaged portion of the specimens exhibited an uneven surface, and the mortar surrounding it displayed a slightly loose consistency. After subjecting the specimens to 600 °C, failure transpired at a rather gradual pace upon reaching the ultimate load. The occurrence of crack formation was accompanied by a substantial release of debris, resulting in an uneven damaged portion. The aggregate was not sheared off but mostly manifested the detachment of mortar and aggregate particles.

At ambient temperature, the effect of incorporating a certain volume of BF on the failure process and modes of the specimens was insignificant. Nevertheless, a notable alteration in the failure mechanism of the specimens that contained BF was observed upon exposure to 300 °C. In particular, many vertical fissures emerged in the central region of the specimen's surface upon reaching the ultimate load. The manifestation of this phenomenon was more pronounced in the specimens that undergone exposure to 600 °C. This phenomenon arose due to the degradation of the internal mortar of the specimens after exposure to elevated temperature. This degradation decreased the bond strength between the aggregate and the mortar, increasing the likelihood of crack formation under the influence of the splitting load. In this particular scenario, the bridging mechanism of fiber effectively halted the propagation of fractures, causing the cracks to alter their trajectory of growth. The failure modes of specimens under various replacement ratios were indistinguishable.

4.1.2 Flexural failure

Fig. 3 displays the modes of flexural failure observed in the partial specimens. The failure process and modes of the specimens exposed to 300 °C were identical to those observed at room temperature. No discernible alterations

were observed on the exterior of the specimens during initial loading. Nevertheless, the specimens promptly underwent a bifurcation after increasing the applied load to its maximum capacity, resulting in the formation of a fracture between the two concentrated stresses. The affected area displayed an extremely even surface that was mostly characterized by the detachment of the aggregate and the mortar, with occasional instances of aggregate shearing [33]. After exposure to 600 °C, the specimens exhibited a reasonably gradual failure upon reaching the ultimate load. The occurrence of crack formation was accompanied by a substantial release of debris, resulting in an uneven surface in the affected area and the absence of aggregate shearing. The primary factor that contributed to the failure was the displacement of the mortar and the aggregate. After the application of an excessive load, certain specimens modified with BF exhibited numerous cracks located between the two focused loads. However, the ultimate failure modes did not demonstrate significant differences. The distinction among the failure modes of the specimens at different replacement ratios was not fully elucidated.

(c) δ = 100% λ = 0 kg·m^{-3} T = 600 °C

Fig. 3. Flexural failure modes of partial specimens.

4.2 Analysis of influential parameters

4.2.1 Splitting tensile strength

The measured values of the splitting tensile strength of the specimens after exposure to elevated temperature are provided in Table 4. Fig. 4 illustrates the extent of variance in the splitting tensile strengths of partial specimens across different variation factors [34].

(a) δ = 50% λ = 2 kg·m^{-3} T = 300 °C

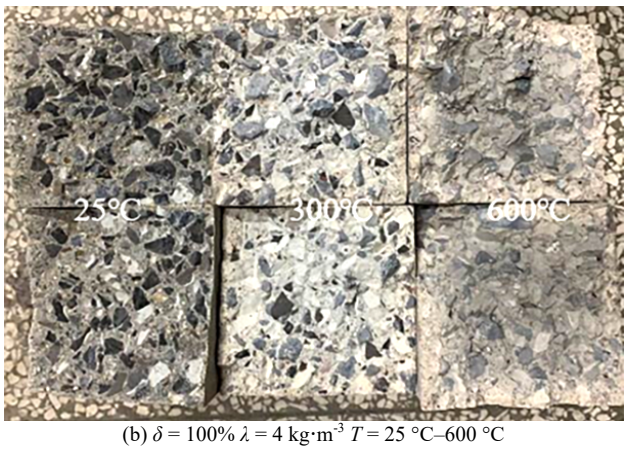

(b) δ = 100% λ = 4 kg·m^{-3} T = 25 °C–600 °C

For specimens with replacement ratio as the only variable parameter, splitting tensile strength tends to decrease as replacement ratio increases. When fiber dosage and temperature remain constant, an increase in replacement ratio from 0% to 50% results in a decrease in splitting tensile strength ranging from 6.4% to 18.6%. Furthermore, when replacement ratio is increased from 50% to 100%, the observed reductions in splitting tensile strengths remain consistent, i.e., ranging from 2.06% to 11.4% for the same fiber dosage and temperature. This finding further demonstrates that the presence of flaws inherent in RCA exerts a comparable effect on the splitting tensile strength of the specimens. Moreover, when temperature increases, the effect of different replacement ratios on splitting tensile strength diminishes gradually. After exposure to 600 °C, splitting tensile strength exhibits a drop of approximately 4% as replacement ratio increases. This finding indicates that the effect of temperature on splitting tensile strength is more pronounced than that of replacement ratio.

In the case of specimens where the only variable parameter is fiber dosage, splitting tensile strength exhibits a progressive increase with increasing fiber dosage. When replacement ratio and temperature remain constant, splitting tensile strength is increased from 5.1% to 14.8% as fiber dosage increases within 0-2 kg·m^{-3}. When fiber dosage is increased within 2-4 kg·m^{-3}, while maintaining the same replacement ratio and temperature, the observed improvements in splitting tensile strength fall within the range of 5.3% to 18%. This phenomenon arises as a result of the toughening and crack-resistance properties exhibited by BF. During the specimen dissection procedure, the application of BF efficiently inhibits the propagation of fractures, using a certain amount of energy and consequently enhancing splitting tensile strength. Nevertheless, the splitting tensile strength of the specimens only exhibits a 5% increase as BF dosage is increased after exposure to 600 °C. One possible explanation for this phenomenon is that the mortar becomes loose and porous after being subjected to elevated temperatures. Consequently, the bond force between BF and the mortar matrix diminishes, weakening the bridging action of BF.

The splitting tensile strength of the specimens exhibits a significant decrease when temperature is the only variable parameter. When temperature is increased within 25 °C to

300 °C, splitting tensile strength experiences a drop ranging from 38.5% to 45.2%, while maintaining the same replacement ratio and fiber dosage. When temperature is increased within 300 °C to 600 °C, splitting tensile strength experiences a drop ranging from 57.4% to 62.3%, while maintaining the same replacement ratio and fiber dosage. The decline in the splitting tensile strength of the specimens after exposure to elevated temperatures exhibits a considerable reduction within each temperature interval. This phenomenon arises due to the deterioration of the interior mortar of the specimens, resulting in a loss of cohesion and increased brittleness during exposure to elevated temperatures. In addition, the bond strength between the aggregate and mortar diminishes. Furthermore, the specimens under consideration exhibit a significant presence of internal microcracks, resulting in a substantial reduction of their splitting tensile strength.

Table 4. Splitting tensile strength of the specimens after exposure to elevated temperatures.

Specimens	f_{st} (MPa)	Specimens	f_{st} (MPa)	Specimens	f_{st} (MPa)
R-0-0-25	2.83	R-0-0-300	1.55	R-0-0-600	0.66
R-0-2-25	3.19	R-0-2-300	1.78	R-0-2-600	0.75
R-0-4-25	3.44	R-0-4-300	1.96	R-0-4-600	0.79
R-50-0-25	2.61	R-50-0-300	1.45	R-50-0-600	0.58
R-50-2-25	2.83	R-50-2-300	1.62	R-50-2-600	0.61
R-50-4-25	3.05	R-50-4-300	1.80	R-50-4-600	0.72
R-100-0-25	2.31	R-100-0-300	1.42	R-100-0-600	0.54
R-100-2-25	2.55	R-100-2-300	1.55	R-100-2-600	0.59
R-100-4-25	2.78	R-100-4-300	1.68	R-100-4-600	0.65

Note: f_{st} denotes splitting tensile strength. $f_{st}=2F/\pi A$, where F refers to the ultimate load, and A refers to the cross-sectional area.

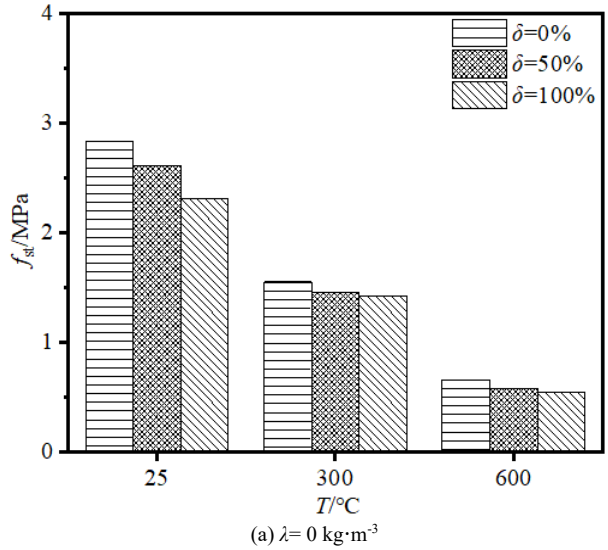

(a) λ= 0 kg·m^{-3}

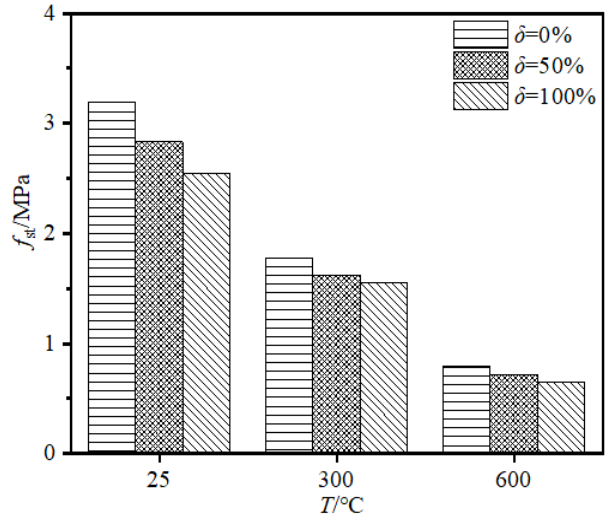

(b) λ= 2 kg·m^{-3}

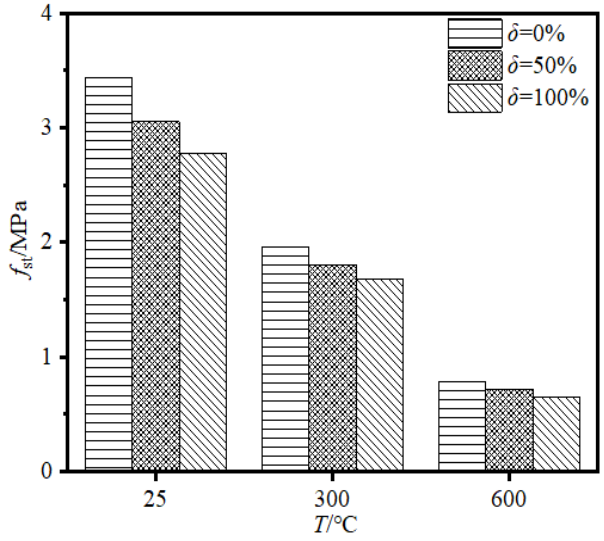

(c) λ= 4 kg·m^{-3}

Fig. 4. Variation magnitude of the splitting tensile strength of partial specimens for various variation parameters.

4.2.2 Flexural strength

Table 5 provides the measured flexural strengths of the specimens after their exposure to increased temperatures. Fig. 5 illustrates the extent of variance in the flexural strength of partial specimens across several variation parameters.

For specimens with replacement ratio as the only variable parameter, flexural strength tends to decrease as replacement ratio increases. When fiber dosage and temperature remain constant, flexural strength exhibits a drop ranging from 3.6% to 18% as replacement ratio increases from 0% to 50%. When fiber dosage and temperature remain constant, flexural strength demonstrates a drop ranging from 7% to 21.2% as replacement ratio is increased within 50% to 100%. This phenomenon arises due to the presence of significant initial damage in the RCA, including microcracks, which progressively accumulate with increasing replacement ratio and directly affect the flexural strength of the specimens.

In the case of specimens where the only variable parameter is fiber dosage, flexural strength exhibits a progressive increase when fiber dosage is increased. When replacement ratio and temperature remain constant, flexural

strength experiences an increase ranging from 4.5% to 26.9% as fiber dosage is increased within 0 kg·m^{-3} to 2 kg·m^{-3}. When replacement ratio and temperature remain constant, flexural strength increases from 1.8% to 16.25% as fiber dosage is enhanced within 2 kg m^{-3} to 4 kg m^{-3}. This finding suggests that the application of BF effectively enhances the flexural strength of the specimens.

When temperature is the only variable parameter, the flexural strength of the specimens exhibits a notable decrease after elevated temperature exposure. When temperature is increased within 25 °C to 300 °C, flexural strength declines by around 53.8% to 58.6%, while maintaining the same replacement ratio and fiber dosage. When temperature is increased within 300 °C to 600 °C, flexural strength experiences a drop ranging from 52.1% to 65.0%, while maintaining the same replacement ratio and fiber dosage. The decrease in flexural strength of the specimens exhibits a consistent pattern throughout all temperature intervals, with values exceeding 50%. The rationale for this phenomenon is as follows: as temperature increases, microcracks within the specimens undergo expansion, resulting in the accumulation of damage. Consequently, the mortar within the specimens becomes loose and porous, significantly reducing bonding strength associated with the mortar and the aggregate. Ultimately, this decrease in bond force considerably diminishes the flexural strength of specimens.

Table 5. Flexural strength of the specimens after exposure to elevated temperatures.

Specimens	f_b (MPa)	Specimens	f_b (MPa)	Specimens	f_b (MPa)
R-0-0-25	5.2	R-0-0-300	2.2	R-0-0-600	0.9
R-0-2-25	5.5	R-0-2-300	2.3	R-0-2-600	1.1
R-0-4-25	5.7	R-0-4-300	2.6	R-0-4-600	1.2
R-50-0-25	4.8	R-50-0-300	2.1	R-50-0-600	0.8
R-50-2-25	5.3	R-50-2-300	2.2	R-50-2-600	0.9
R-50-4-25	5.4	R-50-4-300	2.4	R-50-4-600	1.0
R-100-0-25	3.9	R-100-0-300	1.8	R-100-0-600	0.6
R-100-2-25	4.6	R-100-2-300	1.9	R-100-2-600	0.8
R-100-4-25	5.0	R-100-4-300	2.1	R-100-4-600	0.9

Note: f_b denotes flexural strength. f_b=FL/bh^2, where F refers to the ultimate load, L refers to the span between supports, b refers to section width, and h refers to section height.

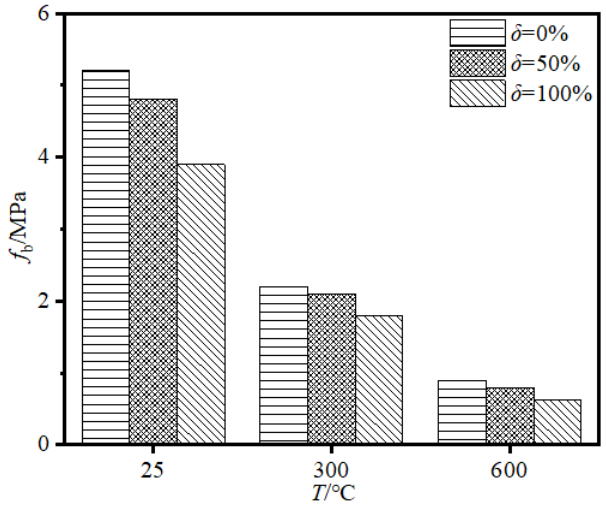

(a) λ= 0 kg·m^{-3}

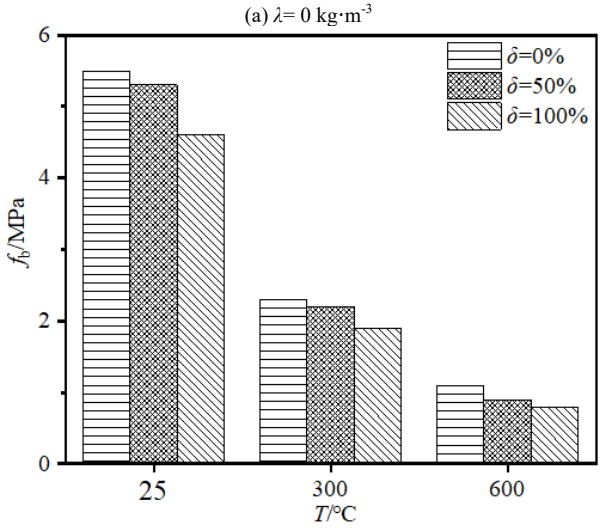

(b) λ= 2 kg·m^{-3}

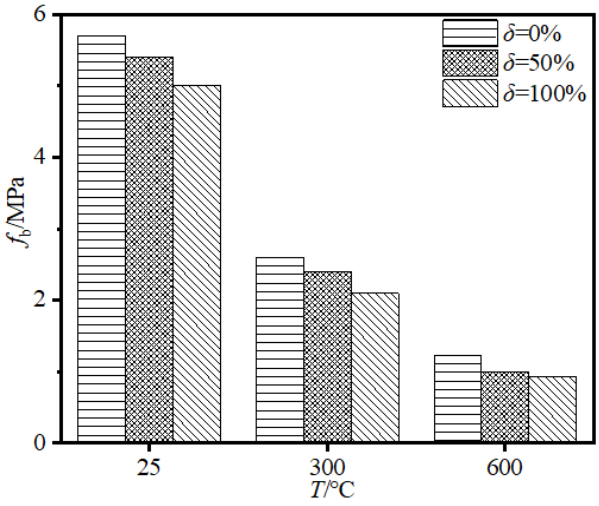

(c) λ= 4 kg·m^{-3}

Fig. 5. Variation magnitude of the flexural strength of partial specimens for various variation parameters.

4.3 Conversion relationships among the strength indexes of BFRRC

4.3.1 Splitting tensile and cubic compressive strengths

RAC has the same low tensile strength as conventional concrete, and its splitting tensile strength correlates with the strength and distribution of aggregate, mortar density, and porosity content. All of which are strongly affected by material performance. In terms of the effect of variation parameters, such as exposure temperature, on material properties, the conversion relationship between f_{st} and f_{cu} is obtained through multiple regression analysis by using the data in Table 4 and cubic compressive strength data from related research [35]. The result is shown in Eq. (1).

$$\begin{cases} f_{st}/f_{cu}^{0.5} = (93.3\lambda - 307.26\delta - 4.994T)\times 10^{-4} + 0.427 \\ R^2 = 0.97 \end{cases} \quad (1)$$

4.3.2 Flexural and cubic compressive strengths

From the information in Table 5 and other research [35], multiple regression analysis is used to find the conversion relationship between f_b and f_{cu}. This step is realized by adjusting for the influences of replacement ratio, fiber dosage, and temperature. The result is shown in Eq. (2).

$$\begin{cases} f_b / f_{cu} = (12.7\lambda - 47.56\delta - 1.25T) \times 10^{-4} + 0.109 \\ R^2 = 0.89 \end{cases} \quad (2)$$

5. Conclusions

The study conducted an indirect tensile strength performance test on BFRRC specimens after exposure to elevated temperatures. The objective was to investigate and analyze the failure modes, factors that influenced strength, and conversion of strength indices. The main conclusions are obtained as following:

(1) The failure mode of the BFRRC specimens is significantly influenced by temperature, with higher temperatures leading to more severe damage to a specimen. The utilization of BF can effectively mitigate potential damage to a specimen. However, the effect of RCA replacement ratio on the overall outcome is not readily discernible.

(2) As the replacement ratio and temperature of RCA increase, the indirect tensile mechanical properties of BFRRC tend to decrease. However, the inclusion of BF can considerably enhance the indirect tensile mechanical properties of BFRRC.

(3) The functional relationship between the conversion values (f_{st}/f_{cu} and f_b/f_{cu}) and the variation parameters is established by analyzing the change pattern of splitting tensile strength with flexural strength under different variation parameters.

Acknowledgements

This work was supported by the Funds for Establishment Project of Double First-Class Disciplines of the Safety and Energy Engineering Department (AQ20230731), the Key Scientific Research Projects of Colleges and Universities in Henan Province (23A560008), and the Henan Province National Science Foundation (222300420446).

References

[1] C. R. Wu, Z. Q. Hong, J. L. Zhang, and S. C. Kou, "Pore size distribution and ITZ performance of mortars prepared with different bio-deposition approaches for the treatment of recycled concrete aggregate," *Cem. Concr. Compos.*, vol. 111, Aug. 2020, Art. no. 103631.

[2] N. Tošić, S. Marinković, T. Dašić, and M. Stanić, "Multicriteria optimization of natural and recycled aggregate concrete for structural use," *J. Clean. Prod.*, vol. 87, pp. 766-776, Jan. 2015.

[3] X. F. Chen and C. J. Jiao, "Microstructure and physical properties of concrete containing recycled aggregates pre-treated by a nano-silica soaking method," *J. Build. Eng.*, vol. 51, Jul. 2022, Art. no. 104363.

[4] M. X. Ma, V. W. Y. Tam, K. N. Le, and R. Osei-Kyei, "Factors affecting the price of recycled concrete: A critical review," *J. Build. Eng.*, vol. 46, Apr. 2022, Art. no. 103743.

[5] N. Russo and F. Lollini, "Effect of carbonated recycled coarse aggregates on the mechanical and durability properties of concrete," *J. Build. Eng.*, vol. 51, Jul. 2022, Art. no. 104290.

[6] K. P. Verian, W. Ashraf, and Y. Z. Cao, "Properties of recycled concrete aggregate and their influence in new concrete production," *Resour., Conserv. Recycl.*, vol. 133, pp. 30-49, Jun. 2018.

[7] M. Elsayed, S. R. Abd-Allah, M. Said, and A. A. El-Azim, "Structural performance of recycled coarse aggregate concrete beams containing waste glass powder and waste aluminum fibers," *Case Stud. Constr. Mater.*, vol. 18, Jul. 2023, Art. no. e01751.

[8] K. Bru, S. Touzé, F. Bourgeois, N. Lippiatt, and Y. Ménard, "Assessment of a microwave-assisted recycling process for the recovery of high-quality aggregates from concrete waste," *Int. J. Miner. Process.*, vol. 126, pp. 90-98, Jan. 2014.

[9] O. Linderoth, and P. Johansson, "A method to determine binder content in small samples of cementitious material using hydrochloric acid and ICP-OES analysis," *Mater. Today Commun.*, vol. 20, Sept. 2019, Art. no. 100538.

[10] V. Spaeth and T. A. Djerbi, "Improvement of recycled concrete aggregate properties by polymer treatments," *Int. J. Sustain. Built Environ.*, vol. 2, no, 2, pp. 143-152, Dec. 2013.

[11] S. C. Kou, B. J. Zhan, and C. S. Poon, "Use of a CO_2 curing step to improve the properties of concrete prepared with recycled aggregates," *Cem. Concr. Compos.*, vol. 45, pp. 22–28, Jan. 2014.

[12] Z. Y. Luo, W. G. Li, V. W. Y. Tam, J. Z. Xiao, and S. P. Shah, "Current progress on nanotechnology application in recycled aggregate concrete," *J. Sustain. Cem.-Based Mater.*, vol. 8, no. 2, pp. 79-96, Mar. 2019.

[13] V. S. Babu, "Strength and durability characteristics of high-strength concrete with recycled aggregate-influence of mixing techniques," *J. Sustain. Cem.-Based Mater.*, vol. 3, no. 2, pp. 88-110, Jan. 2014.

[14] J. J. Zeng, S. P. Chen, Y. Zhuge, W. Y. Gao, Z. J. Duan, and Y. C. Guo, "Three-dimensional finite element modeling and theoretical analysis of concrete confined with FRP rings," *Eng. Struct.*, vol. 234, May. 2021, Art. no. 111966.

[15] N. P. Tran, C. Gunasekara, D. W. Law, S. Houshyar, S. Setunge, and A. Cwirzen, "Comprehensive review on sustainable fiber reinforced concrete incorporating recycled textile waste," *J. Sustain. Cem.-Based Mater.*, vol. 11, no. 1, pp. 28-42, Jan. 2022.

[16] Y. X. Zheng, P. Zhang, Y. C. Cai, Z. Q. Jin, and E. Moshtagh, "Cracking resistance and mechanical properties of basalt fibers reinforced cement-stabilized macadam," *Compos. Part B Eng.*, vol. 165, pp. 312-334, May. 2019.

[17] X. J. Shi, P. Park, Y. Rew, K. J. Huang, and C. Sim, "Constitutive behaviors of steel fiber reinforced concrete under uniaxial compression and tension," *Constr. Build. Mater.*, vol. 233, Feb. 2020,. Art. no. 117316.

[18] Z. R. Wang, G. Ma, Z. H. Ma, and Y. Zhang, "Flexural behavior of carbon fiber-reinforced concrete beams under impact loading," *Cem. Concr. Compos.*, vol. 118, Apr. 2021, Art. no. 103910.

[19] Z. D. Zhu, C. Zhang, S. S. Meng, Z. Y. Shi, S. Z. Tao, and D. Zhu, "A statistical damage constitutive model based on the weibull distribution for alkali-resistant glass fiber reinforced concrete," *Materials*, vol. 12, no. 12, Jun. 2019, Art. no. 1908.

[20] J. A. Sainz-Aja, M. Sanchez, L. Gonzalez, P. Tamayo, G. Garcia del Angel, A. Aghajanian, et al., "Recycled polyethylene fibres for structural concrete," *Appl. Sci.*, vol. 12, no. 6, Mar. 2022, Art. no. 2867.

[21] J. L. Liu, Y. M. Jia, and J. Wang, "Experimental study on mechanical and durability properties of glass and polypropylene fiber reinforced concrete," *Fibers Polym.*, vol. 20, no. 9, pp. 1900-1908, Sept. 2019.

[22] J. Bošnjak, A. Sharma, and K. Grauf, "Mechanical properties of concrete with steel and polypropylene fibres at elevated temperatures," *Fibers*, vol. 7, no. 2, Jan. 2019, Art. no. 9.

[23] Z. N. Li, A. Q. Shen, G. P. Zeng, and Y. C. Guo, "Research progress on properties of basalt fiber-reinforced cement concrete," *Mater. Today Commun.*, vol. 33, Dec. 2022, Art. no. 104824.

[24] I. Taji, S. Ghorbani, J. de Brito, V. W. Y. Tam, S. Sharifi, A. Davoodi, et al., "Application of statistical analysis to evaluate the corrosion resistance of steel rebars embedded in concrete with marble and granite waste dust," *J. Clean. Prod.*, vol. 210, pp. 837-846, Feb. 2019.

[25] E. R. K. Chandrathilaka, S. K. Baduge, P. Mendis, and P. S. M. Thilakarathna, "Structural applications of synthetic fibre reinforced cementitious composites: A review on material properties, fire behaviour, durability and structural performance," *Structures*, vol. 34, pp. 550-574, Dec. 2021.

[26] J. F. Dong, Q. Y. Wang, and Z. W. Guan, "Material properties of basalt fibre reinforced concrete made with recycled earthquake waste," *Constr. Build. Mater.*, vol. 130, pp. 241-251, Jan. 2017.

[27] X. G. Zhang, G. Q. Zhou, P. Xu, L. Fu, D. P. Deng, X. M. Kuang, et al., "Mechanical properties under compression and microscopy analysis of basalt fiber reinforced recycled aggregate concrete," *Materials*, vol. 16, no. 6, Mar. 2023, Art. no. 2520.

[28] N. Shatarat, H. Katkhuda, M. Ayyoub, Y. Al-Hunaiti, and M. S. Abdel Jaber, "Improving bond strength of recycled coarse aggregate concrete using chopped basalt fibers," *Case Stud. Constr. Mater*., vol. 17, Dec. 2022, Art. no. e01449.

[29] X. G. Zhang, X. M. Kuang, F. Wang, and S. R. Wang, "Strength indices and conversion relations for basalt fiber-reinforced recycled aggregate concrete," *DYNA*, vol. 94, no. 1, pp. 82-87, Jan. 2019.

[30] S. P. Li, Y. B. Zhang, and W. J. Chen, "Bending performance of unbonded prestressed basalt fiber recycled concrete beams," *Eng. Struct.*, vol. 221, Oct. 2020, Art. no. 110937.

[31] C. S. Zhang, Y. Z. Wang, X. G. Zhang, Y. H. Ding, and P. Xu, "Mechanical properties and microstructure of basalt fiber-reinforced recycled concrete," *J. Clean. Prod.*, vol. 278, Jan. 2021, Art. no. 123252.

[32] X. F. Chen, S. C. Kou, and F. Xing, "Mechanical and durable properties of chopped basalt fiber reinforced recycled aggregate concrete and the mathematical modeling," *Constr. Build. Mater.*, vol. 298, Sept. 2021, Art. no. 123901.

[33] S. R. Wang, H. G. Xiao, P. Hagan, and Z. S. Zou, "Mechanical behavior of fully-grouted bolt in jointed rocks subjected to double shear tests," *DYNA*, vol. 92, no. 3, pp. 314-320, May 2017.

[34] S. R. Wang, H. G. Xiao, Z. S. Zou, C. Cao, Y. H. Wang, and Z. L. Wang, "Mechanical performances of transverse rib bar during pull-out test," *In. J. Appl. Mech.*, vol. 11, no. 5, Jun. 2019, Art. no. 1950048.

[35] X. Gao, "Research on mechanical properties and micro mechanism of basalt fiber reinforced recycled aggregate concrete after high temperature," M.S., thesis, Sch. of Civil Eng., Henan Polytech. Univ., Jiaozuo, China, 2021.